Gas recognition based on the physicochemical parameters determined by monitoring diffusion rates in microfluidic channels

Ali HOOSHYAR ZARE[1], Vahid GHAFARINIA[2], Sobhan ERFANTALAB[1], Faramarz HOSSEIN-BABAEI[1*]

* Corresponding author: Tel.: +98 (0) 21 88734172; Fax: +98 (0) 21 88768289; Email: fhbabaei@yahoo.com, fhbabaei@kntu.ac.ir
1: Electronic Materials Laboratory, Electrical Engineering Department, K. N. Toosi University of Technology, Tehran 1635-1355, Iran
2: Department of Electrical and Computer Engineering, Isfahan University of Technology, Isfahan, 84156-83111, Iran

Abstract Monitoring the diffusion progress rates of different gases in a microfluidic channel affords their discrimination by the comparison of their temporal profiles in a high-dimensional feature space. Here, we demonstrate gas recognition by determination of their three important physicochemical parameters via a model-based examination of the experimentally determined diffusion rates in two different cross-section channels. The system utilized comprises two channels with respective cross-sectional diameters of 1000 μm and 50 μm. The open end of both channels are simultaneously exposed to the analyte, and the temporal profiles of the diffusion rates are recorded by continuous resistance measurements on the chemoresistive sensors spliced to the channels at their other ends. Fitting the solutions of the diffusion equation to the experimental profiles obtained from the large cross-section channel results in the diffusivity of the analyte. The results of small cross-section channel, however, fit the solutions of a modified diffusion equation which accounts for the adsorption of the analyte molecules to the channel walls, as well. The latter fitting process results in the adsorption parameter for the analyte-channel wall interactions and the population of the effective adsorption sites on the unit area of the walls. The allocation of these three meaningful parameters to an unknown gaseous analyte affords its recognition.

Keywords: Microfluidics, Gas flow, Gas analysis, Gas adsorption, Diffusivity

1. Introduction

Artificial systems mimicking the operational features and quality factors of the mammalian olfaction systems [Firestein, 2001; Persaud et al., 1982; Lewis and Nathan, 2004] are in demand for many industrial and domestic applications. Such compact size, light weight, durable, rugged, user friendly [Hossein-Babaei and Ghafarinia, 2010a; Hossein-Babaei and Amini, 2012] and low cost systems are expected to discriminate among odors and complex gas mixtures [Hossein-Babaei and Amini, 2012; Nakata and Akakabe, 1996] without systematic quantitative analyses. Sensor array-based e-nose systems [Trincavelli and Coradeschi, 2009; Kaur, 2012] satisfy most of the required operational conditions and are, in principle, suitable for these applications, but they generally suffer from the unpredictable [Zhang, 2013; Martinelli et al., 2013; Nicolas, 2007] and predictable [Hossein-Babaei and Ghafarinia, 2010b] drifts of the array components [Vergara, 2012; De Vito et al., 2012], which render the system unreliable and necessitate frequent recalibrations and/or costly sensor array replacements [Coté, 2003; Tomic, 2004; Shah, 2008]. The problem would have been removed if the system could utilize only a single sensor as the device could be recalibrated by a simple test predefined for its recalibration. Unfortunately, the responses of semiconductor gas sensors are mostly non-selective and, hence, fail to afford gas identification.

It has been shown that trace gases in a background of air can be identified by the

determination of their different diffusion rates through a microfluidic channel [Hossein-Babaei and Ghafarinia, 2010a; Hossein-Babaei et al., 2012]. The system utilizes only a single sensor and, hence, its response drifts can be compensated for by performing a simple calibration test. Here, we report simultaneous utilization of two different diameter diffusion channels for the fast extraction of a number of meaningful analyte-related physical parameters which afford analyte recognition.

2. Experimental

The sensing devices utilized are commercially available chemoresistive tin oxide-based chemoresistive gas sensors (SP3-AQ2, FIS Inc., Japan). Two different sensing units are fabricated; sensor A is connected to a bundle of cylindrical channels with internal diameters of 50 µm, while sensor B is connected to a channel of much larger diameter (d=1000 µm). The channels are made of borosilicate glass.

Meter long channels of different cross-sections are made by pulling down from the heated preforms of appropriate shapes, which were cut into predetermined lengths. The fabricated devices are shown in **Fig. 1a-b**. In sensor A the channel is formed out of 425 d=50 µm channels bundled together in a glass capillary cladding, while sensor B comprises a single d=1000 µm channel. The 425 d=50 µm channels have almost the same useful cross-sectional areas as a single d=1000 µm channel.

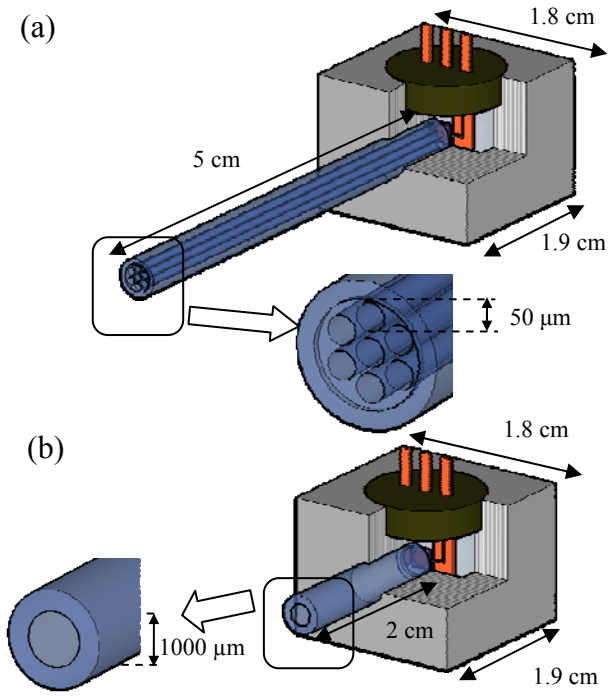

Fig. 1. The schematics of the devices used for gas analyses.

The system used for the experimental work is shown in **Fig. 2**. The apparatus used is a simplified version of the system described in reference [Hossein-Babaei and Ghafarinia, 2010a]. Upon simultaneous exposure of both channels to the contaminated air, the contaminant (analyte) diffuses through the two channels with two different rates (see below) and affects both sensors. The temporal responses of the sensors are related to the diffusion rates of the analyte in their respective channels. Such responses were recorded for different analytes at various concentrations.

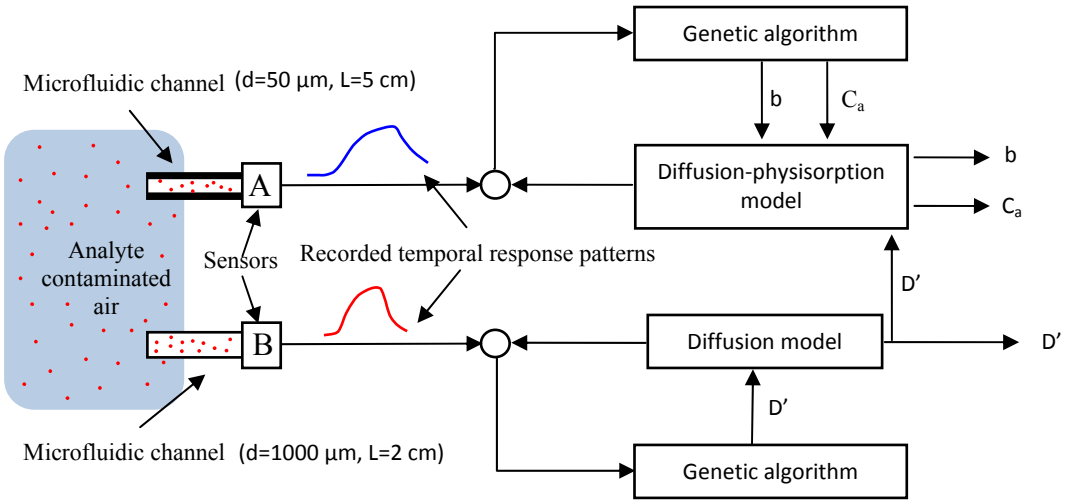

Fig. 2. The schematic diagram depicting the experimental system and the flow chart of the parameter determination process.

The raw responses were filtered for high frequency noise reduction, baseline corrected, and normalized to cover the 0 to 1 magnitude range. The resulted profiles, obtained for six different target analytes, are given in **Fig. 3a-b.**

3. Results and Discussion

The system is schematically defined in **Fig. 4**. The analyte molecules diffuse through the air filled cylindrical channel along the X axis before affecting the gas sensor located at the closed end of the channel. The analyte concentration at the closed end is determined from the solutions of the diffusion physisorption equation [Hossein-Babaei et al., 2014]:

$$\left(1+\frac{4\,C_a}{d}\frac{b}{(1+bC(x,t))^2}\right)\frac{\partial C(x,t)}{\partial t}=D\frac{\partial^2 C(x,t)}{\partial x^2} \qquad (1)$$

Wherein C(x, *t*) is the analyte concentration, D is its diffusivity in air, and C_a and b are physical parameters related to the nature of the analyte and the channel wall [Sommerfeld and Huber, 1999; Sommerfeld, 1992; Hossein-Babaei et al., 2005]. Let's assume, for the sake of argument, that the D of the target analyte examined, is taken from the background literature available [Yaws, 1998].
C_a and b are estimated for each analyte by fitting the solution of (1) to the experimental data obtained from sensor A, as shown in Fig. 5 for an example target analyte. The solutions were determined using MATLAB software "parabolic-elliptic PDE in 1-D" after definition of the initial and boundary values. All fitting processes were carried out using genetic algorithm with minimum mean square error criterion. The optimum fitting conditions are shown in Fig. 5 resulting in the set of fitting parameters given as legend.
In the large diameter channel, physisorption of the analyte to the channel wall surface is negligible and Eq. 1 reduces to the diffusion equation [Crank, 1975]:

$$\frac{\partial C(x,t)}{\partial t}=D\frac{\partial^2 C(x,t)}{\partial x^2} \qquad (2)$$

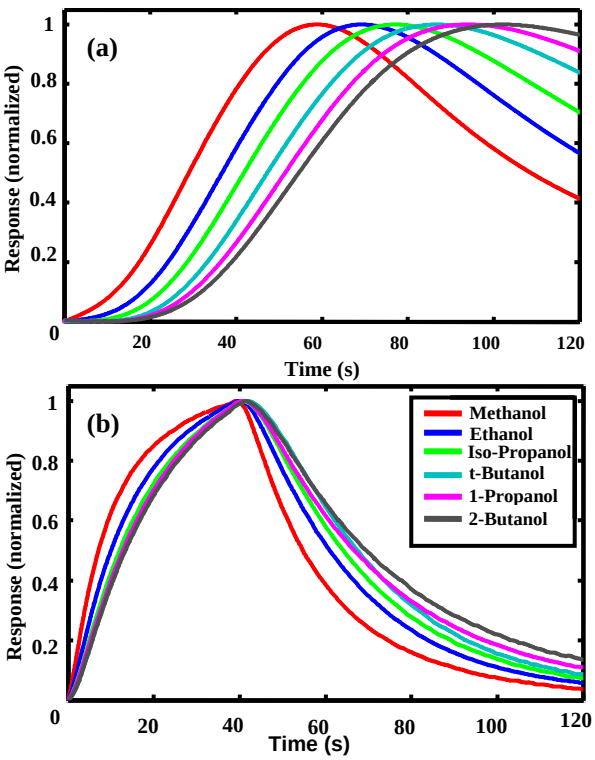

Fig. 3. Responses of a) sensor A and b) sensor B to the stated target gases.

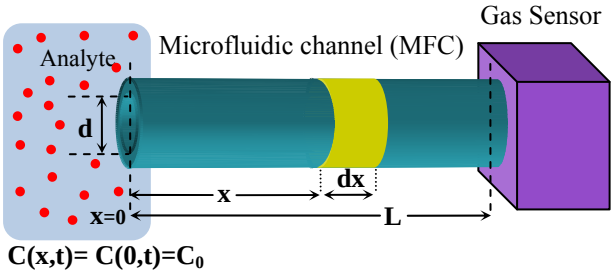

Fig. 4. The schematic presentation of the diffusion-physisoption system defined.

The experimental responses obtained from sensor B attached to the large diameter channel are shown in **Fig. 6**. The fitting of the solutions of (2) to the experimental results are carried out with "parabolic-elliptic PDE in 1-D" technique. The fitting results are shown in **Fig. 6** where the fitting parameter, D', is given as legend.

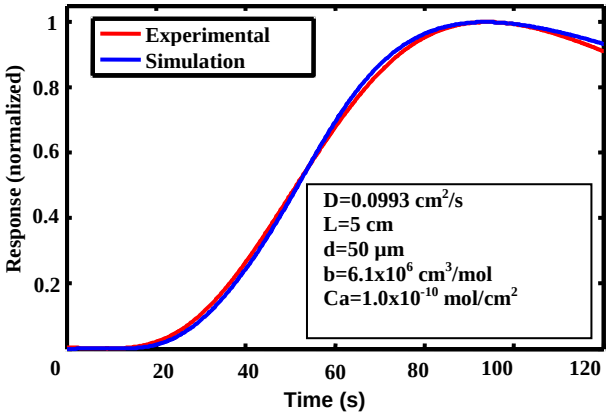

Fig. 5. Fitting the predicted response to that obtained experimentally for 1-propanol using sensor A.

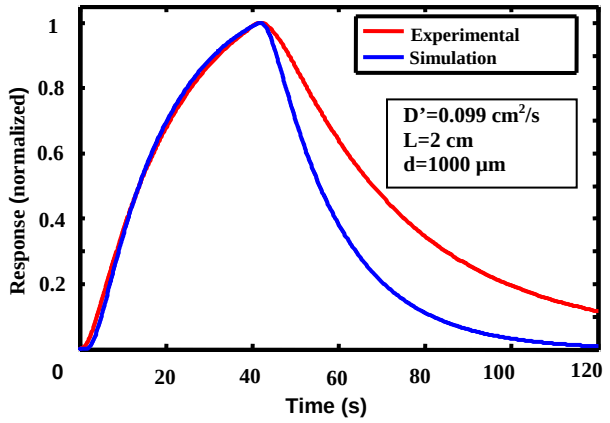

Fig. 6. Fitting of the predicted response to that obtained experimentally for 1-propanol using sensor B.

Table-I. Comparing actual (D) and the estimated (D') values of the diffusivity of different gases examined.

No.	Gas	Formula	D (Diffusion Coefficient) [cm^2/s])	D' (Estimated) [cm^2/s]
1	Methanol	CH_3OH	0.1520	0.154
2	Ethanol	C_2H_5OH	0.1181	0.118
3	Iso-propanol	C_3H_7OH	0.1013	0.102
4	1-propanol	C_3H_7OH	0.0993	0.099
5	Tert-butanol	C_4H_9OH	0.0873	0.088
6	2-butanol	C_4H_9OH	0.0891	0.088

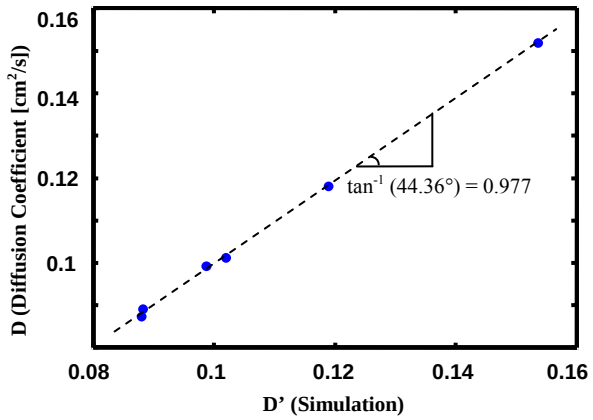

Fig. 7. The relationship between the experimentally obtained diffusivity and the true diffusivity of a number of target analytes plotted based on Table-I.

For each target analyte, the value obtained for D' is compared with its actual diffusivity value available in the literature (Table-I). The correction factor obtained from plotting of D vs. D', given in **Fig. 7,** is 0.977.

An unknown analyte is simultaneously examined with both sensor A and sensor B. The temporal response obtained from sensor B is utilized for the determination of the analyte's D'. This results in the analyte's true diffusivity when multiplied by the correction factor 0.977. The second step is to determine b and C_a values as the fitting parameters of the solutions of (1) to the experimental responses of the sensor A. By inserting the diffusivity of the analyte in (1), the best fitting conditions result in a unique set of b and C_a values for each analyte. As a result of these findings, a set of three parameters, D, b and C_a, is assigned to the unknown analyte.

The above described process was repeated 10 times for each of the 6 target analytes. The concentration of the analyte was different in each run. The extracted parameters D and b are presented in the two-dimensional b-D feature space in **Fig. 8** indicating correct classification of all the analytes examined. Hence, the procedure is capable of discriminating among all the 6 target analytes regardless of their concentrations. Unlike feature spaces resulting from dimensional reduction tools such as the "principal component analysis", the principal axes of the feature space utilized here are of physical meanings related to the nature of the analytes. This is of technical significance as it facilitates prediction of the feature space position of an unexamined analyte; the position of a specific gas in the feature space can approximately be predicted without system training. For the sake of demonstration, the position of iso-butanol

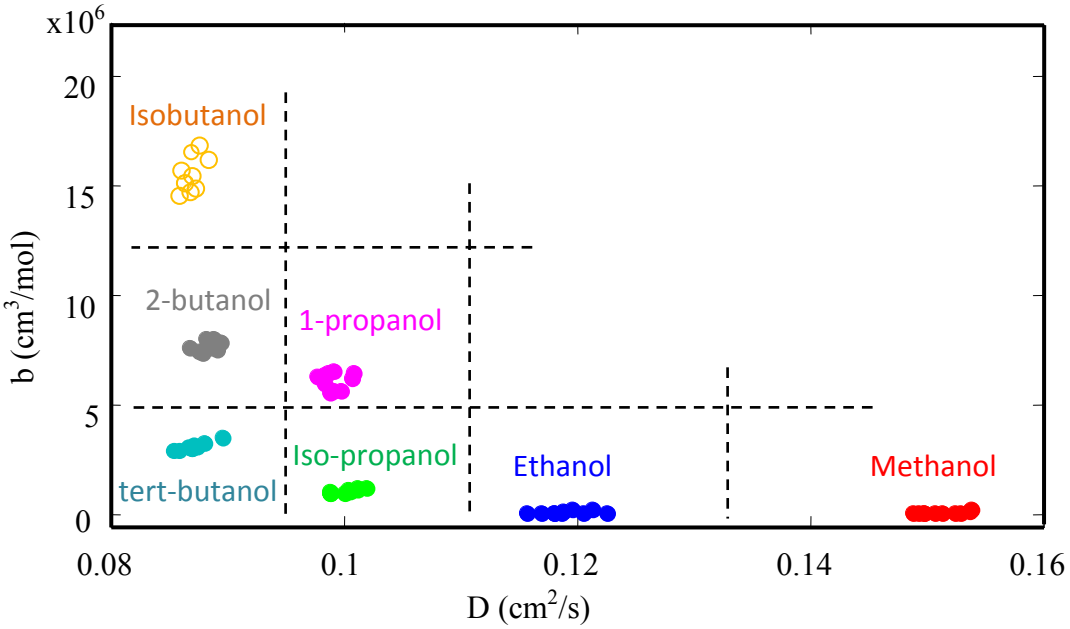

Fig. 8. The presentation of the D and b parameters obtained based on the results of 10 x 7 experimental runs carried out on the stated target analytes at various concentrations indicating 100% correct classification of the analytes. The position of iso-butanol was predicted prior to its test.

vapor was predicted in the feature space shown in Fig. 8; the b and D values obtained in 10 different conditions verified the prediction (see the empty markers in Fig. 8).

4. Conclusions

Recording the progress rates of the diffusion process of a trace gas in two different diameter channels facilitates determination of three independent physical parameters of the trace gas. These parameters determine the position of the analyte in a feature space which can afford its recognition. Correct discriminations among six closely related volatile organic compounds, regardless of their respective concentration in air, were demonstrated.

The significant aspect of the described gas recognition method is utilizing a feature space of physically meaningful principal axes. This allows the prediction of the approximate feature space position of a known gas prior to any system training run.

References

Coté, G.L., Lec, R.M., Pishko, M.V., 2003. Emerging biomedical sensing technologies and their applications. IEEE Sens. J 3, 251-266.

Crank, J., 1975. The Mathematics of Diffusion, 2nd ed. Oxford University Press, New York, 326.

De Vito, S., Fattoruso, G., Pardo, M., Tortorella, F., Di Francia, G., 2012. Semi-Supervised Learning Techniques in Artificial Olfaction: A Novel Approach to Classification Problems and Drift Counteraction. IEEE Sens. J 12, 3215-3224.

Firestein, S., 2001. How the olfactory system makes sense of scents. Nature 413, 211–218.

Hossein-Babaei, F., Amini, A., 2012. A breakthrough in gas diagnosis with a temperature-modulated generic metal oxide gas sensor. Sensors Actuators, B 166–167, 419–425.

Hossein-Babaei, F., Amini, A., 2014. Recognition of complex odors with a single generic tin oxide gas sensor. Sensors Actuators, B 194, 156–163.

Hossein-Babaei, F., Ghafarinia, V., 2010a. Gas analysis by monitoring molecular diffusion in a microfluidic channel. Anal. Chem. 82, 8349–8355.

Hossein-Babaei, F., Ghafarinia, V., 2010b. Compensation for the drift-like terms caused by environmental fluctuations in the responses of chemoresistive gas sensors. Sensors Actuators, B 143, 641–648.

Hossein-Babaei, F., Hemati, M., Dehmobed, M., 2005. Gas diagnosis by a quantitative assessment of the transient responses of a capillary attached gas sensor. Sensors Actuators, B 107, 461-467.

Hossein-Babaei, F., Paknahad, M., Ghafarinia, V., 2012. A miniature gas analyzer made by integrating a chemoresistor with a michrochannel, Lab. Chip 12, 1874-1880.

Kaur, R., Kumar, R., Gulati, A., Ghanshyam, C., Kapur, P., Bhondekar, A.P., 2012. Enhancing electronic

nose performance: a novel feature selection approach using dynamic social impact theory and moving window time slicing for classification of Kangra orthodox black tea (Camellia sinensis (L.) O. Kuntze). Sensors Actuators, B 166-167, 309–319.

Lewis, N.S., 2004. Comparisons between mammalian and artificial olfaction based on arrays of carbon black-polymer composite vapor detectors. Acc. Chem. Res. 37, 663-672.

Martinelli, E., Magna, G., De Vito, S., Di Fuccio, R., Di Francia, G., Vergara, A., Di Natale, C., 2013. An adaptive classification model based on the Artificial Immune System for chemical sensor drift mitigation. Sensors Actuators, B 177, 1017-1026.

Nakata, S., Akakabe, S., Nakasuji, M., Yoshikawa, K., 1996. Gas sensing based on a nonlinear response: discrimination between hydrocarbons and quantification of individual components in a gas mixture. Anal. Chem. 68, 2067–2072.

Nicolas, J., Romain, A.C., Delva, J., 2007. Electronic nose: a promising tool for landfill odour monitoring. Landfill Research Focus.

Persaud, K., George, D., 1982. Analysis of discrimination mechanisms in the mammalian olfactory system using a model nose. Nature, 352-355.

Shah, R., Wang, L., Zhang, Y. 2008. System and method for sensor recalibration. U.S. Patent No. 7, 384-397.

Sommerfeld, M., 1992. Modelling of particle-wall collisions in confined gas-particle flows. Int. J. Multiphase Flow 18, 905-926.

Sommerfeld, M., Huber, N., 1999. Experimental analysis and modelling of particle-wall collisions. Int. J. Multiphase Flow 25, 1457-1489.

Tomic, O., Eklöv, T., Kvaal, K., Haugen, J.E., 2004. Recalibration of a gas-sensor array system related to sensor replacement. Analytica Chimica. Acta. 512, 199-206.

Trincavelli, M., Coradeschi, S., Loutfi, A., 2009. Odour classification system for continuous monitoring applications. Sensors Actuators, B 139, 265–273.

Vergara, A., Vembu, S., Ayhan, T., Ryan, M.A., Homer, M.L., Huerta, R., 2012. Chemical gas sensor drift compensation using classifier ensembles. Sensors Actuators, B 166-167, 320–329.

Yaws, C.L., 1998. Chemical Properties Handbook, McGraw Hill Professional.

Zhang, L., Tian, F., Liu, S., Dang, L., Peng, X., Yin, X., 2013. Chaotic time series prediction of e-nose sensor drift in embedded phase space. Sensors Actuators, B 182, 71–79.